Solid State Science and Technology, Vol. 19, No2 (2011) 150-161
ISSN 0128-7389

STRUCTURAL AND SURFACE CHARACTERIZATION OF COLD DEPOSITED ZINC SULFIDE THIN FILMS

Saafie Salleh [1,*], M.N. Dalimin [2] and H.N. Rutt [3]

[1]*School of Science, Universiti Malaysia Sabah*
88400 Kota Kinabalu, Sabah, Malaysia

[2]*The Vice-Chancellor Office, Universiti Tun Hussein Onn Malaysia*
83310 Batu Pahat, Johor,Malaysia

[3]*Department of Electronics and Computer Science, University of Southampton,*
SO17 1BJ Highfield, England, United Kingdom

**Corresponding author: saafie@ums.edu.my*

ABSTRACT

Zinc sulfide thin films with the thickness of about 0.5 μm were deposited using a thermal evaporation system onto oxidized silicon substrates at cold temperature (T_{cold} = –50 ^oC) and at ambient temperature ($T_{ambient}$ = 25 ^oC). A special substrate holder with a thermoelectric cooler was used to cool the substrates. The crystalline structure and the morphology of the films were investigated by X-Ray Diffraction and atomic force microscopy, respectively. XRD results show that the structure of the cold deposited ZnS thin film was completely amorphous. The ambient deposited ZnS thin film has a mixture of amorphous structure and polycrystalline structure with the preference orientation of (111) plane. The crystallite size of ambient deposited ZnS thin film was about 10 nm as calculated using the Scherrer formula. The AFM analysis revealed that the estimated grain size of cold deposited and ambient deposited ZnS were about 360 nm and 1220 nm, respectively. The surface roughness of the cold deposited ZnS thin film was greater than the surface roughness of the ambient deposited ZnS thin film.

Keywords: Cold deposition; ZnS thin film; crystallite size; grain size; surface roughness;

INTRODUCTION

This paper discusses the fabrication processes and the physical properties of ZnS planar optical thin films deposited at relatively low substrate temperatures. The substrate cooling in cold deposition was achieved using a self-invented thermoelectrically cooled substrate holder. This represents new method for cold depositions of thin films using thermoelectric coolers and avoids using liquid nitrogen [1]. ZnS is a semiconductor with a wide bandgap of about 3.6 eV which makes it suitable as a transparent material in the visible region. ZnS thin films are extensively used for optoelectronics application such as filters, photoelectric cells, display devices and materials for LEDs and lasers.

ZnS exist in two forms, an α-phase (hexagonal wurtzite structure) and β-phase (cubic sphalerite structure) [2].

Many deposition techniques have been used to prepare ZnS thin films, such as sputtering, pulsed laser deposition, chemical vapor deposition, electron beam deposition, thermal evaporation, photochemical deposition and chemical bath deposition [3]. Among these methods, thermal evaporation is the most common method in producing thin film because the advantages of thermal evaporation are due to its stability, reproducibility and high deposition rates. It is well known that the physical properties such as the structure and the surface are generally different from those of the same materials in bulk form.

The temperature of the substrate plays a vital role in determining the structure of an amorphous or polycrystalline for the thermally deposited thin films. In general, covalently bonded materials such as semiconductors produced either amorphous structures at low substrate temperatures or polycrystalline structures at higher temperatures [4]. The propagation losses in ZnS thin films must be minimized for waveguide application. The high loss in polycrystalline ZnS waveguides are due to the combination of surface scattering and bulk scattering at the crystalline grain boundaries [5]. Therefore, a small grain size is necessary for a reduction of surface roughness and allows a reduction of surface scattering [6]. The smallest grain size of ZnS can be found in its amorphous thin films and can be prepared by depositing ZnS on the cold substrate. It was reported that the propagation losses of ZnS waveguides as a function of substrate temperature. The propagation loss is minimized when the deposition was executed at the substrate temperature of –50 ^{o}C [7].

The purpose of this work is to investigate the effect of the substrate cooling on the physical properties of ZnS thin films. The structural characteristics and the surface roughness of the films are studied and compared to the ambient deposited films. The samples are produced with thermal evaporation with a thermoelectrically cooled substrate holder. The structural and surface characterizations are done using X-ray diffractometer and atomic force microscopy, respectively.

EXPERIMENTAL DETAILS

Sample preparation
Thin films of ZnS were deposited using Edwards (Auto 306) thermal evaporation system. The system pressure was monitored with both Penning gauge and Pirani gauge while the foreline pressure was monitored with a Pirani gauge. The system was regularly pumped down to a base pressure of less than 5 X 10^{-7} Torr. The substrate cooling was achieved using a thermoelectrically cooled substrate holder. The cooling process is simply done by setting the appropriate low voltage of the thermoelectric device. The substrate cooler is operated without liquid nitrogen and is stabled at –50 ^{o}C. Cold deposition was performed at the substrate temperature of –50 ^{o}C and ambient deposition was performed at the substrate temperature of 25 ^{o}C. Substrate temperatures

are measured with a chromel/alumel thermocouple attached directly to the substrate with indium solder [8].

Before each deposition, the substrate was blown with hot air (120 ^{o}C to 150 ^{o}C) for about 10 minutes. This is to ensure that the substrate surface free from water vapour and dust residuals. During this preheating process, the thermoelectric cooler (TEC) was in operation (V_{app} = 3.5 volts) to prevent high temperature damage on the TEC. By applying this procedure, ZnS thin film was found to stick better and was very stable on the substrate. Without preheating, ZnS thin films could be detached easily from the substrate. The source material was ZnS (pieces, 3 – 12 mm) with the purity was approximately 99.999%. The source material was then filled up in the alumina crucible until approximately three quarter full. Fresh source material was used in every deposition to maintain the purity and stoichiometric consistency. The chamber door was closed and the system was pumped. The liquid nitrogen trap was filled and the system was pumped down until the base pressure is reached.

At this stage, the deposition procedures depend on whether cold deposition or ambient deposition was performed. For cold deposition, the TEC power supply was switched ON and was set up to a voltage of 3.5 V. The cold deposition was carried out when the substrate temperature was stabled at –50 ^{o}C. For ambient deposition, no substrate cooling was required and the deposition was performed whenever vacuum level was satisfied. The substrate temperature of ambient deposition was measured and found stabled at about 25 ^{o}C. Once the proper deposition settings were adjusted and recorded, the ZnS source materials was slowly heated up by increase the current of the crucible heater. When the deposition rate of 0.50 nm/s was achieved and stabled at $\pm$ 0.05 nm/s, the shutter was opened. Depositions were carefully performed using the same parameters until the thickness of 0.5 μm was obtained.

X-ray diffractometer (XRD)
XRD is a rapid analytical technique primarily used for phase identification of a crystalline material and can provide information on crystallity, orientation, lattice constants and phase of crystals. X-ray diffraction patterns of the samples were recorded using Panalytical X'Pert Pro diffractometer with Cu Kα radiation (λ = 0.15418 nm) source over the diffraction angle 2θ between 25° and 80°.

If the sample is single crystal or polycrystalline then these X-rays will be scattered from successive planes. Generally the scattering from these planes will be out phase. There will be angles however for which the constructive interference takes place so there is a large signal from the detector. So, diffraction peaks are observed because reflected x-rays interfere constructively from parallel planes within crystal. Those peaks only occur when the Bragg law

$$m\lambda = 2d\sin\theta \qquad (1)$$

is satisfied; where m is the diffracted order, λ is the X-ray wavelength, d is the plane

separation and θ is the incident angle of the X-rays. If the sample is amorphous or polycrystalline with no preferred orientation then the diffraction peaks will not appear as the X-rays are totally scattered.

Atomic force microscopy (AFM)
AFM is a surface analytical technique used to capture high resolution images of a surface. AFM used to study ZnS thin films grown by atomic layer epitaxy and found the technique was appropriate to investigate the surface of deposited ZnS thin films [9]. Atomic force microscopy measurements were carried out with an ARIS-3300 AFM (Burleigh Instruments, Inc., USA) operated in taping mode.

AFM studies were carried out to evaluate both the grain size and surface roughness of ZnS thin films. The AFM images were acquired and analyzed using True Image SPM software. This software communicates through the data acquisition board. The surface analysis of the software menu was used to obtain statistical information about the image [11]. The root mean square (RMS) roughness of the surface is given by:

$$R_{rms} = \sqrt{\frac{1}{N}\sum_{i}^{N}\left(Z_i - Z_{avg}\right)^2} \quad (2)$$

RESULTS AND DISCUSSION

Structural characterization
Figure 1 shows XRD diffraction spectrum of the ambient deposited ZnS thin film. It is observed that the ambient deposited sample have one intense peak from ZnS film at 28.8^o, which corresponds to the (111) reflection. It is also observed that one weak and broad peak at around 49.0^o, which corresponds to (220) reflection. The results show that the ambient deposited sample is microcrystalline with the preference of (111) plane and mixed with amorphous structure.

Figure 2 shows XRD diffraction spectrum of the cold deposited ZnS thin film. The intensity of the peaks clearly decreases which suggests that the cold deposited sample is less preferentially oriented than the ambient deposited sample. The main peak of the ZnS film at 28.8^o became weak and broadened and the second peak at 49.0^o disappeared completely. The crystallinity of the cold deposited ZnS thin film deteriorates and become amorphous. ZnS films with wide peaks on the XRD pattern were amorphous [11].

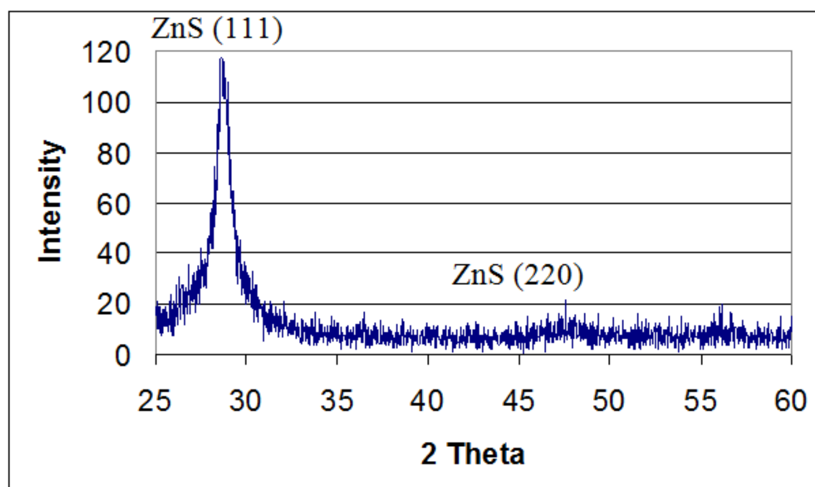

Figure 1: XRD diffractogram of the ambient deposited ZnS thin film

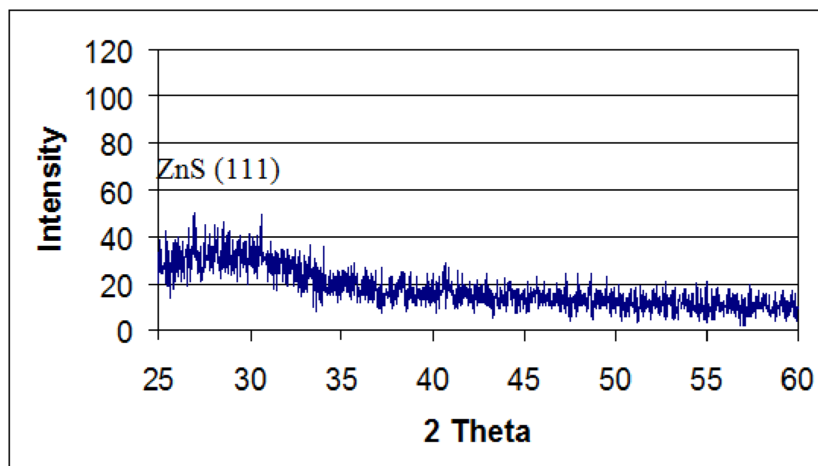

Figure 2: XRD diffractogram of the cold deposited ZnS thin film

The comparison of observed values of the ambient deposited ZnS thin film, the cold deposited ZnS thin film and standard values for ZnS (Powder Diffraction Data by The Joint Committee on Powder Diffraction, 1985, Cards No. 77-2100) is showed in Table 1. The diffraction peaks due to ZnS (110) and ZnS (220) planes corresponds to sphalerite-type ZnS in cubic form. The polycrystalline structure of the ambient deposited ZnS thin film and the amorphous structure of the cold deposited ZnS thin film were in line with the published works. XRD spectra of ZnS thin films prepared at various substrate temperatures showed the highest peak diffraction intensity at 2θ of 28.6^{o} with the preferential orientation of crystallinity to (111) plane of cubic structure [2]. Recently, it was reported that low temperature (less than 300°C) growth of ZnS results in a cubic structure of the thin films [12].

Table 1: Comparisons of standard values of ZnS and observed values for ambient and cold deposited ZnS films. (* indicates that the peak is weak and broadened)

Standard ZnS (PDF77-2100)	Ambient deposited ZnS thin film	Cold deposited ZnS thin film
2-theta (hkl)	2-theta (hkl)	2-theta (hkl)
28.910 (111)	28.88 (111)	*28.88 (111)
48.111 (220)	*48.111 (220)	- -
57.101 (311)	- -	- -

Surface characterization

The 2-D AFM micrography and the surface cross section of the ambient deposited and the cold deposited ZnS thin films are shown in Figure 3 and Figure 4, respectively. These images clearly show that the grains of the ambient deposited ZnS are bigger than the cold deposited ZnS.

The AFM image of the ambient deposited ZnS thin film consists of bigger grains that are randomly distributed. The ambient deposited ZnS thin film has larger grain size as compared to cold deposited ZnS thin film. This suggests that at ambient temperature, ZnS film growth mechanism proceeds through agglomeration of islands (nuclei). The coalescence of the small grains leads to the formation of bigger grains in the thin film along with improved crystallinity as observed from the XRD analysis. The AFM image of the cold deposited ZnS thin film consisted of smaller grains that are more uniformly distributed. The cold deposited ZnS thin film thin film composed of many smaller grains. This implies that the agglomeration of the islands was limited at cold substrate temperature. Depositions at low temperature reduce adatom mobility and significantly influence the film structure. The low temperature deposited ZnS thin films were characterised by the present of columnar grains and the composition of a large number of grains with various sizes [13].

ISSN 0128-7389

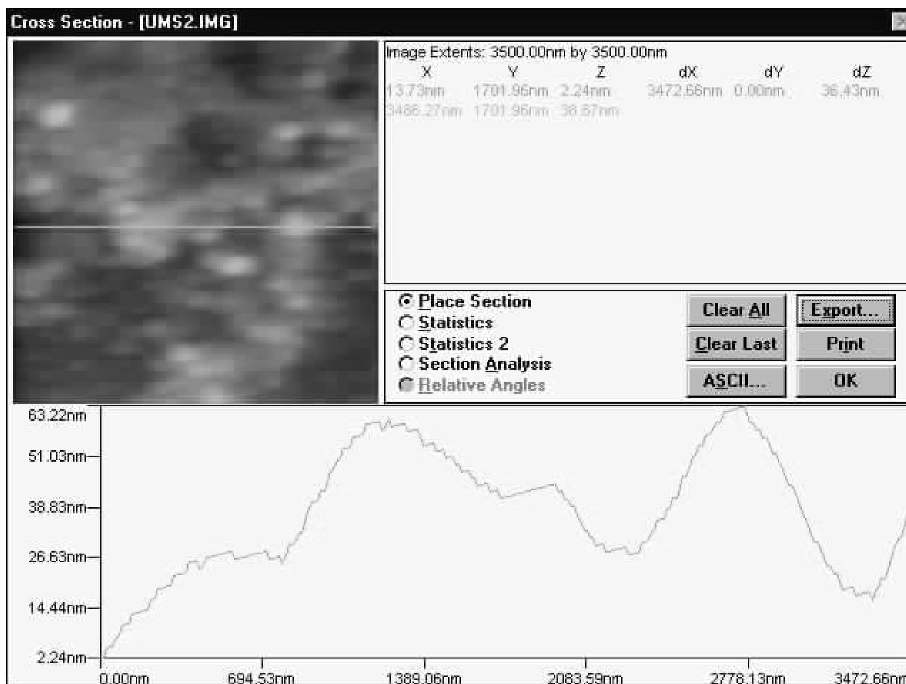

Figure 3: 2-D AFM micrography and surface cross section of the ambient deposited ZnS thin film

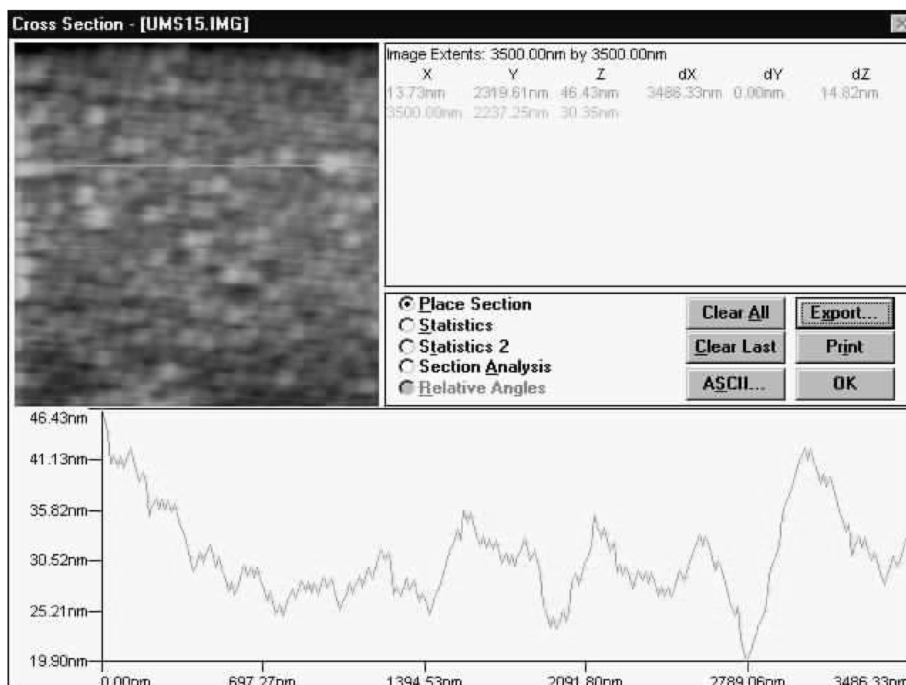

Figure 4: 2-D AFM micrography and surface cross section of the cold deposited ZnS thin film

Using the cross sectional analysis of the AFM images, the average grain size can be estimated using the line method

$$d = 1.5\frac{L}{N} \tag{3}$$

where L is the line length and N is the number of the grains along the line [14, 15]. The grain sizes of the ambient deposited and cold deposited ZnS thin films are listed in Table 2. The average grain size of the ambient deposited ZnS thin film is in the order of 1220 nm whereas the average grain size of the cold deposited ZnS thin film is in the order of 360 nm. These estimated grain sizes were consistent with the structures that were observed from the AFM images. The grains of the cold deposited ZnS thin film were about three times smaller than the ambient deposited thin film.

In order to obtain more structural information, the average crystallite size of the ambient deposited ZnS thin film can be calculated using the Scherrer equation

$$D = \frac{K\lambda}{\beta Cos\theta} \tag{4}$$

where λ is the X-ray wavelength, β is FWHM of the ZnS (111) diffraction peak at 2θ, and θ is the Bragg diffraction angle [16, 17]. The crystallite shape is assumed in round shape (spherical), therefore the shape factor, K of 0.9 is chosen. Referring to the ZnS (111) peak (figure 1), the calculated mean crystallite size of the ambient deposited ZnS thin film is in the order of 10 nm. Zhau-Hong *et al*. [19] found that the crystallite size of room temperature deposited ZnS films was about 20 nm. Wu *et al*. [3] reported that the crystallite size increases from 24 to 31 nm as the thickness increases from 0.3 to 1.2 μm.

The crystallite size of the ambient deposited ZnS thin film is much smaller compare to its grain size. The grains of the ambient deposited ZnS thin film were composed of many fine ZnS crystallites. As expected, the crystallization at this temperature is limited for low temperature deposition. No crystallite is detected in cold deposited ZnS thin film and it was probably due to its amorphous phase. Ruffner *et al*. reported that ZnS thin films deposited at the substrate temperature of -50°C was corresponded to quenching of crystallinity (1989). The ZnS films formed at temperatures lower than -50°C were exhibited less crystallinity and were in amorphous state [19].

The 3-D images of the surfaces ZnS thin films were done by capturing for three different scan areas that were 3.5 μm x 3.5 μm, 7.0 μm x 7.0 μm and 14.0 μm x 14.0 μm for surface roughness analysis. The 3.5 μm x 3.5 μm 3-D images of the ambient deposited and the cold deposited ZnS thin film surfaces are shown in Figure 5 and Figure 6, respectively.

Table 2: Comparison of crystallite size of the ambient deposited ZnS thin film and the grain sizes of the ambient and cold deposited ZnS thin films

Crystallite size of the ambient deposited ZnS thin film (nm)	Grain size of the ambient deposited ZnS thin film (nm)	Grain size of the cold deposited ZnS thin film (nm)
~ 10	~ 1220	~ 360

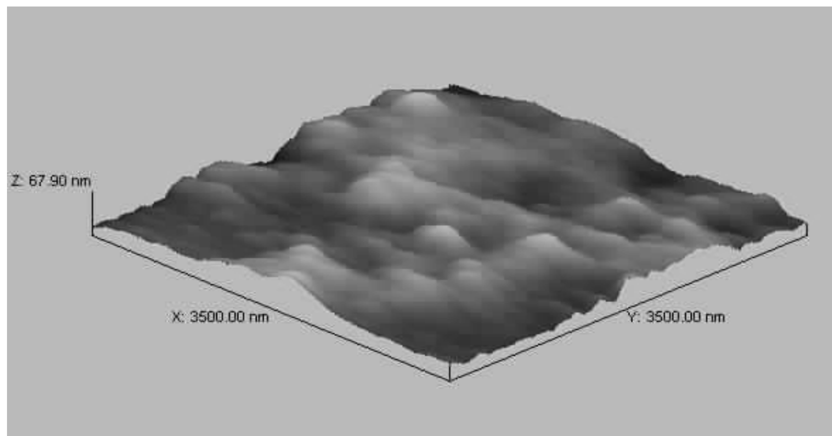

Figure 5: 3-D AFM micrography of ambient deposited ZnS thin film with scan area of 3.5 μm x 3.5 μm

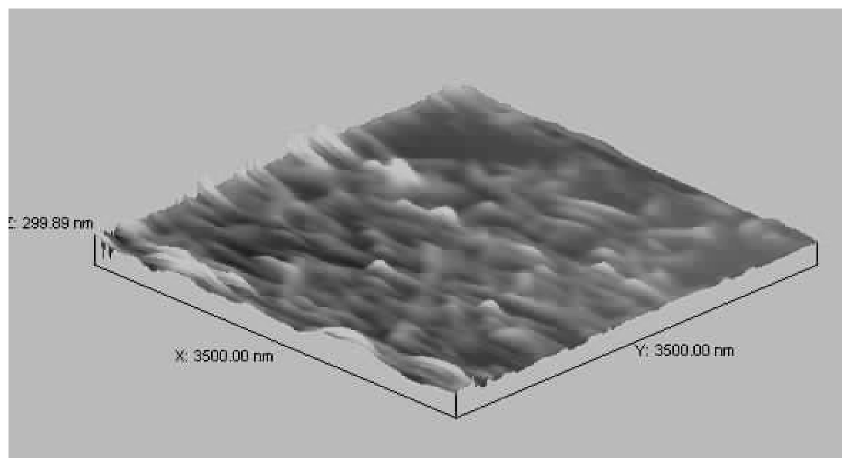

Figure 6: 3-D AFM micrography of cold deposited ZnS thin film with scan area of 3.5 μm x 3.5 μm

Referring to the scales of Z-axis in Figure 5 and Figure 6, it is observed that the surface of ambient deposited ZnS thin film is much flatter than the surface of cold deposited ZnS thin film. Detailed surface roughness of ZnS thin films was calculated based on Equation 2 by using computer software of the microscope control. The values of rms surface roughness of ZnS thin film samples are listed in Table 3. The value of surface roughness of both ambient deposited and cold deposited thin films were consistent for different scan areas. This trend indicates that the surfaces topography of the ZnS thin film samples were uniform.

Table 3: Surface roughness of ambient and cold deposited ZnS thin films

	Surface roughness, R_{rms} (nm)	
Scan area	Ambient deposited ZnS thin film	Cold deposited ZnS thin film
3.5 μm x 3.5 μm	10.28	39.88
7.0 μm x 7.0 μm	10.45	34.40
14.0 μm x 14.0 μm	10.33	35.52

The rms surface roughness for the ambient deposited ZnS thin film were 10.28 nm, 10.45 nm and 10.33 nm for the scanned areas of 3.5 μm x 3.5 μm, 7.0 μm x 7.0 μm, 14.0 μm x 14.0 μm, respectively. The rms surface roughness for the cold deposited ZnS thin film were 39.88 nm, 34.40 nm and 35.52 nm for the scanned areas of 3.5 μm x 3.5 μm, 7.0 μm x 7.0 μm, 14.0 μm x 14.0 μm, respectively. The surface roughness of the cold deposited ZnS thin film was consistently greater (about three times) than the ambient deposited ZnS thin film. The greater value of the surface roughness of the cold deposited ZnS thin film can associated with large amount of fine grains with different sizes distributed randomly all over the surface, which might have corresponded to the amorphous phase.

From the grain size estimation and the surface roughness analysis of the ZnS thin films, the thin film growth mechanism can be predicted. The surface morphology of both the ambient and the cold deposited ZnS thin films had many islands. For the ambient deposited ZnS thin film, the grains are larger because the film growth proceeds through agglomeration of islands. For the cold deposited ZnS thin film, the growths of island were limited and therefore many smaller grains are observed. Low substrate temperature immobilizes or freezes adatoms on the substrate where they impinge and prevent them from diffusing. The growth mechanism in both cases was islands growth where the ZnS adatoms were easily bound to each other and diffusions on the cold substrate were limited.

CONCLUSION

The cold deposited ZnS thin film was completely in amorphous state as concluded from the X-ray diffractogram. However, the ambient deposited ZnS thin film was

microcrystalline with the preferred plane of ZnS (111). The crystallite size of ambient deposited ZnS thin film for this particular plane is about 10 nm as calculated using Scherrer's equation.

The cold deposited ZnS thin film had significantly smaller grains as compared to the ambient deposited ZnS thin film. The grain size of cold deposited ZnS thin film was about three times smaller than ambient deposited ZnS thin film. The surface roughness of cold deposited ZnS thin film was greater (about three times higher) than the ambient deposited ZnS thin film.

REFERENCES

[1] Saafie Salleh, Abdullah Chik, M. N. Dalimin, and H. N. Rutt, *Borneo Science*. **17** (2005) 55-61
[2] M. Y. Nadeem, W. Ahmed and M. F. Wasiq, *Journal of Research (Science)*. **16** (2) (2005) 105-112
[3] X. Wu, F. Lai, L. Lin, J. Lv, B. Zhuang, Q. Yan and Z. Huang. *Applied Surface Science*. **254** (20) (2008) 6455-6460
[4] M. Ohring, *The Material Science of Thin Films.* (Academic Press Incorporated, New York 1992)
[5] M. D. Himel, and T. C. Kimble, *Applied Optics*. **32** (18) (1993) 3306-3311
[6] B. Wong, P.E. Jessop and A.H. Kitai, *Journal of Applied Physics,* **70** (3) (1991) 1180-1184
[7] J. A. Ruffner, M.D. Himel, V. Mizrahi, G.I. Stegeman, and U.J. Gibson. *Applied Optics,* **28** (24) (1989) 209-214
[8] Saafie Salleh, "Fabrication and characterization of zinc sulfide optical waveguides using thermoelectrically cooled substrate holder" (Ph.D. Thesis, Universiti Malaysia Sabah, 2010)
[9] J. Ihanus, M. Ritala, M. Leskela, T. Prohaska, R. Resch, G. Friedbacher, and M. Grasserbauer, *Applied Surface Science* **120** (1997) 43-50
[10] Burleigh Instruments, *Personal Atomic Force Microscope Operating Manual.* (Burleigh Instruments Incorporated, New York, 1994)
[11] Z. Limei, X. Yuzhi, and L. Jianfeng, *Journal of Environmental Sciences Supplement,* **S77-S79** (2009) 77-79
[12] V. L. Gayou, B. Salazar-Hernanddez, M. E. Constantino, E. Rosendo-Andres, T. Diaz, R. Delgado-Macuil and M. Rojas-Lopez, *Vacuum.* **15** (2009) 1-4
[13] B. Maiti, P. Gupta, A. B. Maiti, S. Chaudhuri and A. K. Pal, *Materials Chemistry and Physics,* **39** (1995) 167-173
[14] A. Saynatjoki, J. Riikonen, H. Lipsanen and J. Ahopelto, *Journal of Material Sciene: Materials in Electronics,* **14** (2003) 417-420
[15] T. A. Carbone, "Transition metal doped chalcogenides lasers." *Proceeedings of the 1999 IEEE/SEMI Advanced Semiconductor Manufacturing Conference,* New York, 1999, 359-364.
[16] B. E. Warren, *X-Ray Diffraction.* (Dover Publication, New York, 1990)

[17] H. P. Klug and L. E. Alexander, X-Ray Diffraction Procedures for Polycrystalline and Amorphous Materials, 2nd edition. (Wiley, New York 1974)
[18] L. Zhao-Hong, W. Yu-Jiang, C. Mou-Zhi, C. Zhen-Xiang, S. Shu-Nong and H. Mei-Chun, *Acta Physica Sinica,* **7** (3) (1998) 209-213
[19] Y. P. V. Subbaiah, P. Pratap and K. T. R. Reddy, *Applied Surface Science,* **253** (2006) 2409-2415